



OPEN

Optimization and modelling of magnesium oxide (MgO) photocatalytic degradation of binary dyes using response surface methodology

Hyeong Kwang Benno Park^{1,5}, Pushpendra Kumar^{2,5}, Imen Kebaili³, Imed Boukhris³, Yun Hwan Joo¹, Tae Hyun Sung¹ & Anuruddh Kumar⁴✉

Textile industry dye effluent contains a mixture of different kinds of dyes. Many times, photocatalysis is targeted as a solution for the treatment of dye effluent from the textile industry. Many researches have been published related to the photocatalysis of single textile dyes but in the real-world scenario, effluent is a mixture of dyes. Magnesium oxide (MgO) is used as a photocatalyst to treat a mixture (binary solution) of Methylene blue (MB) and Methylene violet (MV) along with individual MB and MV dyes in this article. MgO shows remarkable photocatalytic activity at about 93 and 88% for MB and MV dye in binary solution within 135 min. Furthermore, to study the influence of process parameters, experiments are designed with the help of the central composite design (CCD), and Response surface methodology (RSM) is used to study the interactions between parameters. For this study, five parameters are selected i.e., Photocatalyst dosage, initial concentration of both dyes, time of exposure to the light source, and pH of the binary solution. The photocatalytic process is also optimized and finally optimization of process parameters is validated with an experiment. The result of the validation experiment is very close to the predicted photocatalytic activity.

Keywords Magnesium oxide (MgO), Photocatalysis, Binary dye, Parametric study, Parameter optimization, Central composite design (CCD), Response surface methodology (RSM)

Textile industries are using dyes in their process production. These dyes are very toxic to the environment ecosystem^{1,2}. Textile industries discharge wastewater effluent directly into the environment. These wastewater effluents contain complex structured compounds that are difficult to biodegrade. These complex structured organic substances are toxic which makes dyes a threat to the human body. Researchers have developed some methods to tackle this problem. Methods are adsorption³, coagulation^{4,5}, flocculation⁶. Photocatalysis is also a method that uses a photocatalyst material that is activated in the sunlight. These materials are stable, abundant, safe, and highly preferred as they are sustainable, non-hazardous, and economical. Metal oxides have been used in various applications such as electronics, catalysts, and biomedicine^{7,8}. Many metal oxides (eg., TiO₂⁸, ZnO⁹, Fe₂O₃¹⁰, and WO₃¹¹) have properties such as nontoxicity, high activity, chemical stability, and low cost and have been used as a photocatalyst material for dye degradation. Catalytic mechanisms of these materials have also been documented¹². Nowadays magnesium oxide (MgO) has caught attention in various applications such as catalytic¹³, electronics¹⁴, and biomedical¹⁵ because of its unique physicochemical properties, low toxicity, and inexpensive properties. The application of MgO is very widespread in various fields such as adsorption¹¹, catalysis¹⁶, antibacterial material¹⁷, paint¹⁸, and superconductors¹⁹. Researchers have made some attempts^{13,14,20-24} to use MgO as a photocatalyst material for the degradation of various dyes in aqueous solution.

¹Department of Electrical Engineering, Hanyang University, Seoul 04763, South Korea. ²Indian Institute of Technology Mandi, Mandi, Himachal Pradesh 175005, India. ³Department of Physics, Faculty of Science, King Khalid University, P.O. Box 9004, Abha, Saudi Arabia. ⁴Center for Creative Convergence Education, Hanyang University, Seoul 04763, South Korea. ⁵These authors contributed equally: Hyeong Kwang Benno Park and Pushpendra Kumar. ✉email: anuruddh07@hanyang.ac.kr

Organic complex structured compounds such as methylene violet (MV), methyl orange (MO), methylene blue (MB), and rhodamine B (RhB) are the most hazardous and important dyes effluent from the textile industry^{25–28}. Most of the researchers use one of these dyes to evaluate the photocatalysis process. But more importantly, in the real-world scenario effluent from the textile industry contains a mixture of dyes so a mixture of dyes is more relevant to consider for photocatalysis. Some of the researchers have tried a mixture of dyes (binary dye) to evaluate the photocatalysis activity by using different combinations of dyes e.g. MO/RhB²⁹, MO/MB^{29,30}, and MB/RhB³¹. Furthermore, one thing is to be noted the textile industry effluent contains a mixture of dyes with different individual dye concentrations at variable pH. So, this concentration and pH of effluent are also important parameters to consider while designing any catalyst material. The amount of catalyst and time of catalysis are the other important parameters because they are directly associated with the effectivity of photocatalysts.

Conventionally, these process parameters are analyzed by holding a parameter constant while varying other parameters. The holding of a parameter at an unspecified constant level does not show the combined effect of all the parameters involved. This method is very time-consuming and requires a lot of experiments to optimize all parameters. By together optimizing all the influencing parameters using statistical experimental design, such as Response Surface Methodology (RSM)⁷, these limitations of the conventional technique can be avoided. Using statistical experimental design approaches in the development of photocatalytic processes can lead to several benefits, including improved photocatalytic activity, reduced process variability, closer confirmation of the output response to nominal and target requirements, and reduced development time and overall costs. Many researchers have used this Response Surface Methodology a statistical experimental design approach to optimize and understand the behavior of process parameters^{32,33}. It is well well-established method and widely reported for photocatalysis experiments. However, it has not been explored for MgO as a photocatalyst for the degradation of binary dye.

This research article is related to the use of Magnesium Oxide (MgO) as a photocatalyst material for the degradation of a mixture of dyes (Binary dye). A mixture of Methylene Blue (MB) and Methyl Violet (MV) is used for this study because a mixture of dyes is more relevant in the case of textile effluent. Furthermore, the effect of process parameters is also analyzed and optimized with the help of Response Surface Methodology (RSM). Five parameters (Factors) such as pH of the solution, irradiation time, catalyst dosage, initial MB dye concentration, and initial MV dye concentration are selected for this study. To analyze these parameters, the experiments are designed with the help of Central Composite Design (CCD) by Design Expert (version 13) software. The quality of fitting of the model and the effect of individual and interaction of parameters are evaluated by analysis of variance (ANOVA). The parameters are optimized for the highest photoactivity and also validated by experiment.

Material and methods

Magnesium oxide (MgO) powder was purchased from Adnano Technologies Pvt. Ltd., India. The absorption spectra of MB and MV dyes were collected using the Shimadzu UV-2600 UV-Vis spectrophotometer. MgO photocatalyst was drop cast in ethanol on a silicon wafer and Scanning electron microscope (SEM) images of MgO powder were recorded using FE-SEM Inspect™S50.

The photocatalysis experimental setup contains a visible light source, a reaction beaker, a magnetic stirrer, and a box. The reaction beaker was kept on a magnetic stirrer and a visible light source was placed above 15 cm from the upper surface of the dye solution. The visible light source was from Havells company and of 15 W power rating. The whole experimental setup was kept inside a box to avoid any type of unwanted radiation.

All the experiments were conducted in a 20 ml solution of dyes of known initial concentration, photocatalyst dosage, and pH. The pH of the dye solution was adjusted by 0.1 M HCl and 0.1 M NaCl solution. The dye aqueous solution was put in the dark for 5 h to establish the adsorption equilibrium of MB, and MV dyes on the photocatalyst surface area. After establishment, the dye solution was centrifuged at 3000rpm for 3 min to separate the photocatalyst and then analyzed by UV-visual spectrophotometer. Dye along with the photocatalyst used for analysis was again mixed with the dye solution. The dye solution was exposed to a light source. After the specified period dye solution was brought out again and was centrifuged at 3000rpm for 3 min. After this process, the mixture was again analyzed and subsequently, degradation efficiency was calculated via the following Eq. (1).

$$P = (C_0 - C_t) / C_0 \times 100 \quad (1)$$

Where P is the degradation efficiency (%), C_0 is the initial concentration of the dye solution and C_t is the concentration of dye after a specific period.

The photocatalytic activity was evaluated for individual MB and individual MV dyes and a mixture of both dyes (binary dye). The initial concentration of single MB and MV dyes was 10 mg/L at natural pH and the amount of photocatalyst (MgO) used was 5 g/L. Photocatalytic activity was also evaluated for the binary mixture of MB and MV dyes. The volumetric ratio of MB and MV dyes was taken as 1:1 with 10 mg/L initial concentration of each dye. The amount of photocatalyst used was 5 g/L.

Interaction between given parameters (factors) was studied by RSM and experiments were designed by central composite design (CCD) with the help of Design Expert version 13 software. A CCD with five levels and five factors was selected. These factors were X1: Photocatalyst dosage (g/L), X2: time of exposure (minutes), X3: MB dye initial concentration (mg/L), X4: MV dye initial concentration (mg/L), and X5: pH of the dye solution. CCD can evaluate a quadratic model recognize the main effective factors interact them with a minimum number of required experiments and optimize multiple variables^{34,35}. The ranges of factors along with the low, center, and high points can be seen in Table 1.

The CCD design suggested 27 individual experiments in two blocks and a small design. It is shown in Table 2. The polynomial equation [(Eq. 2)] was used for the mathematical relationship between independent

S.No	Factors	Unit	Low	Centre	High
1	X1: Photocatalyst dosage	g/L	3	5	7
2	X2: time of exposure	min	75	135	195
3	X3: MB dye initial concentration	mg/L	5	10	15
4	X4: MV dye initial concentration	mg/L	5	10	15
5	X5: pH		3	5	7

Table 1. Factors and their ranges for CCD matrix.

Run	Block	Factors					Responses	
		X1: Photocatalyst dosage (g/L)	X2: Time (min)	X3: Initial MB concentration (mg/L)	X4: Initial MV concentration (mg/L)	X5: pH	R1: MB dye degradation efficiency (%)	R2: MV dye degradation efficiency (%)
1	1	5	135	10	10	6	77	82
2		7	75	5	15	8	48	52
3		3	195	5	15	8	77	92
4		3	195	15	5	8	57	67
5		5	135	10	10	6	78	82
6		7	195	15	5	4	70	73
7		5	135	10	10	6	79	83
8		7	195	5	15	4	77	56
9		7	75	15	5	8	21	26
10		7	195	5	5	8	67	62
11		5	135	10	10	6	70	77
12		3	195	15	15	4	58	75
13		3	75	5	5	4	53	56
14		3	75	15	15	8	22	45
15		7	75	15	15	4	28	42
16	2	5	135	10	10	6	67	73
17		5	135	10	19	6	70	85
18		5	135	10	10	9.6	71	78
19		1.3	135	10	10	6	6	24
20		5	135	19	10	6	40	53
21		8.6	135	10	10	6	71	75
22		5	135	10	10	2.3	66	77
23		5	135	10	10	6	56	68
24		5	135	0.9	10	6	98	83
25		5	26	10	10	6	6	8
26		5	244	10	10	6	88	89
27		5	135	10	0.9	6	75	77

Table 2. CCD matrix and responses.

parameters^{36–38}. Analysis of variance (ANOVA) was used to evaluate the quality of the fitted model. The significance of the model was determined by p-value and f-value³⁹.

$$\text{Log}_{10}(R) = \beta_0 + \sum_{i=1}^6 \beta_i X_i + \sum_{i,j=1}^6 \beta_{ij} X_1 X_2 + \sum_{i=1}^6 \beta_{ii} X_i^2 + \varepsilon \quad (2)$$

Some experiments suggested by CCD (Table 2) showed combined degradation efficiency (MB and MV dyes) more than optimized values. While designing experiments by CCD, it is used to take some axial points beyond predefined ranges. Axial points are taken to observe results beyond predefined ranges and correlate them with experiments done in the range. Experiments run 24 and 26 are the axial points taken by CCD which are beyond predefined ranges. In an experiment run 24, a concentration of MB dye was taken for the axial point. As the concentration of MB dye was considerably less than the predefined range, it showed higher photodegradation efficiency than the predicted value. Experiment run 27 was also an axial point taken by CCD. CCD took time of reaction as an axial point. As the time of reaction was considerably higher than the predefined range, it showed higher photodegradation efficiency. Experiments 19 and 21 are also similar types of experiments.

Results and discussion

Scanning electron microscope (SEM) images are shown in Fig. 1. The big particle shown in Fig. 1b is an MgO particle and the background is ethanol which was used for sample preparation (drop cast). It can be concluded from the images that MgO powder particles were in specific shapes and sizes. The average size of the powder particle was 2.5 μm . X-ray diffraction is not shown here as this material was purchased from the market and the same is directly used in the present experiments.

The photocatalytic activity was evaluated for single MB and single MV dyes. For this purpose, the initial concentration of individual single MB dye and individual single MV dyes was 10 mg/L at natural pH and the amount of photocatalyst (MgO) was 5 g/L. MB and MV dye absorption characteristic peak was found at 663 and 587 nm respectively. The effect of photocatalysis was determined by monitoring characteristic peak. During the photocatalysis process, the intensity of the absorption peak was decreased which indicated a decrement in the concentration of dyes (Fig. 2). Figure 2a and Fig. 2b show the absorption Vs wavelength plot depicting this decrement for individual single MB and MV dyes respectively. MgO photocatalyst showed 78% degradation in 120 min when an individual single MB dye aqueous solution was used for photocatalysis (Fig. 2a). However, individual single MV dye showed an 87% degradation in 270 min (Fig. 2b). Many researches have been published to report the photocatalytic activity of MgO/modified MgO photocatalysts^{40–45}.

The absorption Vs wavelength plot of individual single MB, single MV dye at a concentration of 10 mg/L, and binary solution of MB and MV dye with a volumetric ratio of 1:1 at a concentration of 10 mg/L are shown in Fig. 3a. It can be observed from the plot that after mixing both dyes in equal amounts (the volumetric ratio is 1:1), the intensity of the absorption peaks of binary dyes decreased. It indicated that the concentration of both dyes decreased. When two dyes were mixed, the amount of solvent increased because it came from both dyes. As the amount of solvent in the binary mixture of dyes increased and the amount of MB and MV dye was constant, the concentration of MB and MV dye in the binary mixture decreased.

The photocatalytic activity was evaluated for the binary mixture of MB and MV dyes. MB and MV dye absorption peaks were found at 663 nm and 598 nm respectively. The effect of photocatalysis was determined by monitoring absorption characteristic peaks. During the photocatalysis process, the intensity of the absorption

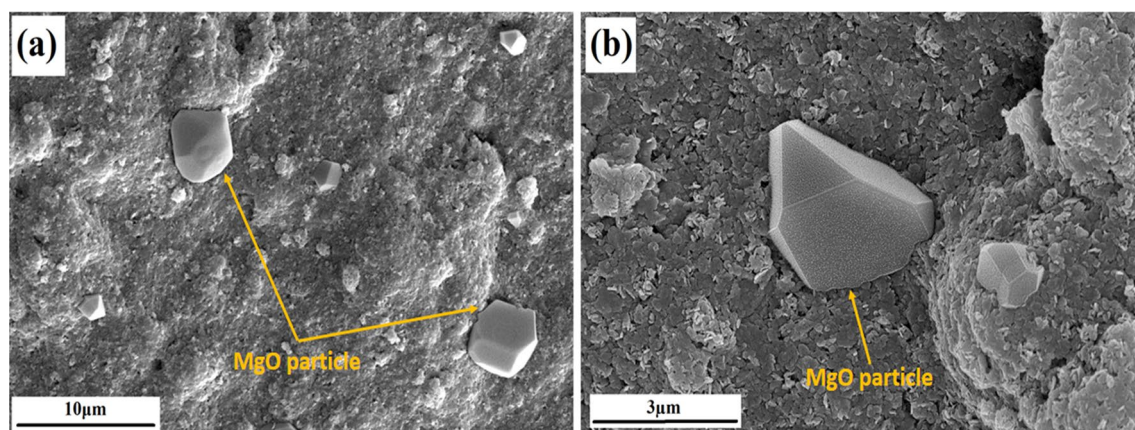


Figure 1. Scanning electron microscopy images of (a) a MgO particle and (b) a single particle of MgO.

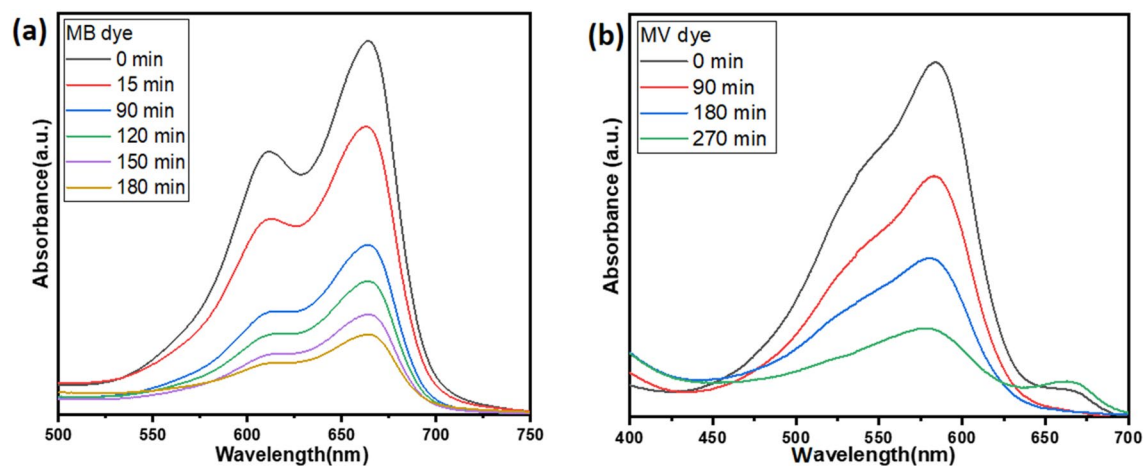


Figure 2. UV visible spectra of Photocatalysis of (a) MB dye and (b) MV dye at 5 g/L MgO powder dosage, 100 mg/L dye concentration, and natural pH.

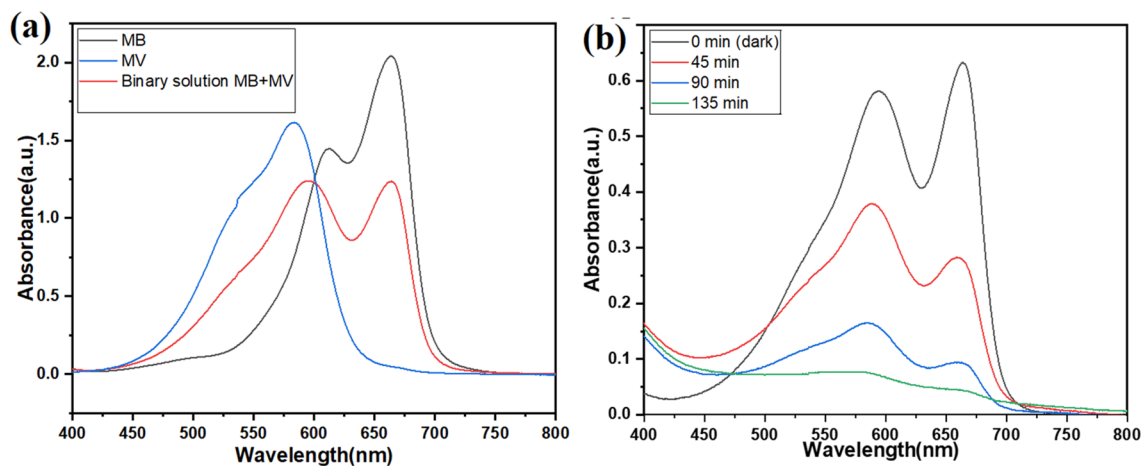


Figure 3. UV-visible spectra: (a) absorption spectra for a single and binary mixture of MB and MV dye (10 mg/L) and (b) absorption spectra for photocatalysis of 10 mg/L of each dye for 135 min, 5 g/L MgO nanoparticle dosage and natural pH.

characteristics peak was decreased which indicated that the concentration of dyes was also decreasing (figure 3b). MB and MV dyes showed 93 and 88 % degradation efficiency in binary solution within 135 min respectively.

Figure 4a shows the degradation efficiency of MgO photocatalyst (C/C_0) versus time plots when an individual single MB and MV dyes and binary solutions of MB and MV dyes were used for photocatalysis. Figure 4a revealed that MB dye in a binary mixture of dyes is degrading fastest whereas individual single MV dye degrades slowest. Figure 4a also revealed that both dyes are degrading faster when they are in binary dye solution. It implies that when photocatalytic reactions of both dyes take place in the binary solution then both reactions help each other to increase the rate of reaction.

L-H equation has been often used for the modelling of photocatalytic degradation. It was expressed by a first-order kinetic model [Eq. (3)].

$$\ln(C_0/C_t) = kt \quad (3)$$

Here C_0 is the initial concentration, C_t is the concentration of dye solution after the t time-period of light illumination for the photocatalytic experiment., and k (min^{-1}) is the rate constant of the photocatalytic reaction. Empirical data was fitted for single MB and MV dye with and without photocatalyst along with MB and MV dyes in binary dye solution. Figure 4b shows (C_0/C_t) versus time graph with rate constant of reaction. The reaction rate constant for MB dye in the binary mixture of dyes is the highest whereas the same is the lowest in the case of single MV dye solution.

The electron (e^-) and hole (h^+) were generated by the ejection of electrons from the valance band to the conduction band when the MgO catalyst powder was illuminated. These electrons and holes migrate to the surface of the MgO catalyst powder particle and make an active site for advanced oxidation reactions. Free radicals are generated by the interaction of e^- and h^+ with the H_2O and O_2 molecules at active sites. The HOO free radical

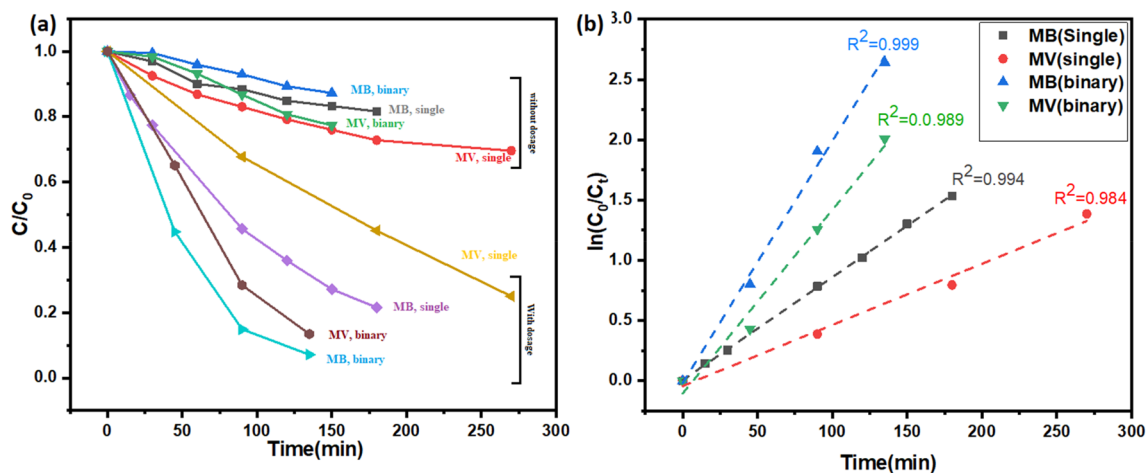


Figure 4. (a) C/C_0 versus time plots and (b) $\ln(C_0/C_t)$ versus time plots for MB and MV single dyes and a mixture of both dyes.

was generated by the reduction reaction of superoxide anion (O_2^-). Now, the HOO free radical reacts with e^- and hole h^+ and generates H_2O and it consumes free energy and releases the hydroxyl radicals. Moreover, this h^+ in the valance band reacts with H_2O molecule and generates hydroxyl radicals⁴⁶. These generated hydroxyl radicals attack on dye molecule break down the structure of the dye molecule and produce H_2O and other byproducts⁴⁷.

CCD was used to design experiments to study the influences of selected parameters (factors). The experiments along with their degradation efficiencies are shown in Table 2. The degradation activity and parameters fitted in Eq. (2) by software and analyzed by Analysis of variance (ANOVA) to evaluate the quality of the fitted equation. The significance of the fitting was determined by p-value and f-value. Table 3 illustrates the five-factor CCD matrix and fitting results of the degradation of the binary dye solutions.

To find the influencing factors and the interactions between factors, analysis of variance (ANOVA) was used^{48–50}. In Table 3, p-values and f-values are indicated for individual coefficients in the equation. A p-value less than 0.0001 shows the significant effect and statistical significance of results at a 95% confidence level. Whereas, the F-values for the model are 114.62 and 191.48 for MB and MV dye in binary solution respectively. The lack of fit (LOF) of the Fitted models for photodegradation of binary dye with MgO as photocatalyst is not significant which indicates the reliability of the fitted model and all values indicate that the model is perfectly fitted and can be used for further analysis.

The values of adjusted and predicted R^2 were evaluated (Table 4) and found around 0.98 and 0.83, and 0.99 and 0.90 for MB and MV dyes (respectively) in the binary solution. This is an indication of a good relation between the observed and predicted values. The signal-to-noise ratio (adequate precision) was 39.8 and 62.5 for MB and MV respectively. The final fitted equation for MB dye degradation is shown in Eq. (4) in terms of coded factors. Whereas, Eq. (5) shows the fitted equation for the degradation of MV in the binary solution in terms of coded factors.

Source	MB dye					MV dye				
	DF	SS	MS	F	P	DF	SS	MS	F	P
Block	1	0.0400	0.0400			1	0.0116	0.0116		
Model	16	2.52	0.1576	114.62	<0.0001	17	1.37	0.0805	191.48	<0.0001
X1	1	0.6369	0.6369	463.26	<0.0001	1	0.1529	0.1529	363.53	<0.0001
X2	1	0.9133	0.9133	664.26	<0.0001	1	0.6461	0.6461	1535.87	<0.0001
X3	1	0.1381	0.1381	100.44	<0.0001	1	0.0230	0.0230	54.75	<0.0001
X4	1	0.0038	0.0038	2.74	0.1323	1	0.0016	0.0016	3.82	0.0864
X5	1	0.0033	0.0033	2.44	0.1531	1	0.0000	0.0000	0.0665	0.8030
X1X2	1	0.1484	0.1484	107.91	<0.0001	1	0.1048	0.1048	249.13	<0.0001
X1X3	–	–	–	–	–	1	0.0024	0.0024	5.68	0.0444
X1X5	1	0.0331	0.0331	24.08	0.0008	1	0.0018	0.0018	4.21	0.0742
X2X3	1	0.0681	0.0681	49.50	<0.0001	1	0.0078	0.0078	18.52	0.0026
X2X4	1	0.0168	0.0168	12.20	0.0068	1	0.0017	0.0017	3.98	0.0812
X3X4	1	0.2696	0.2696	196.11	<0.0001	1	0.1517	0.1517	360.73	<0.0001
X3X5	1	0.1330	0.1330	96.73	<0.0001	1	0.0925	0.0925	219.82	<0.0001
X4X5	1	0.2017	0.2017	146.74	<0.0001	1	0.1399	0.1399	332.48	<0.0001
X1 ²	1	0.3800	0.3800	276.40	<0.0001	1	0.0858	0.0858	204.02	<0.0001
X2 ²	1	0.3191	0.3191	232.10	<0.0001	1	0.3324	0.3324	790.28	<0.0001
X4 ²	1	0.0163	0.0163	11.83	0.0074	1	0.0094	0.0094	22.24	0.0015
X5 ²	1	0.0089	0.0089	6.51	0.0311	1	0.0052	0.0052	12.25	0.0081
Residual	9	0.0124	0.0014			8	0.0034	0.0004		
Lack of fit	5	0.0079	0.0016	1.41	0.3809	4	0.0023	0.0006	2.25	0.2259
Pure error	4	0.0045	0.0011			4	0.0010	0.0003		
Cor total	26	2.57				26	1.38			

Table 3. ANOVA for a quadratic model with \log_{10} transformation for photocatalysis of binary dye mixture.

Dye	Standard deviation	Mean	CV (%)	PRESS	R ²	Adjusted R ²	Predicted R ²	Adequate precision
MB	0.0371	1.70	2.18	0.4125	0.9951	0.9864	0.8372	39.8467
MV	0.0205	1.78	1.15	0.1265	0.9975	0.9923	0.9079	62.5551

Table 4. Model fitting statistics.

$$\begin{aligned} \text{Log}_{10}(R_1) = & 1.84 + 0.2766X_1 + 0.3312X_2 - 0.1048X_3 - 0.0173X_4 + 0.0201X_5 - 0.1983X_1X_2 - 0.0937X_1X_5 \\ & + 0.1248X_2X_3 + 0.0619X_2X_4 + 0.2544X_3X_4 + 0.1744X_3X_5 \\ & + 0.2148X_4X_5 - 0.1341X_1^2 - 0.1229X_2^2 + 0.0277X_4^2 + 0.0206X_5^2 \end{aligned} \quad (4)$$

$$\begin{aligned} \text{Log}_{10}(R_2) = & 1.87 + 0.1396X_1 + 0.2870X_2 - 0.0435X_3 + 0.0143X_4 - 0.0019X_5 - 0.1759X_1X_2 \\ & + 0.0241X_1X_3 - 0.0229X_1X_5 + 0.0436X_2X_3 - 0.0222X_2X_4 + 0.1925X_3X_4 \\ & + 0.1502X_3X_5 + 0.2032X_4X_5 - 0.0637X_1^2 - 0.1254X_2^2 + 0.0210X_4^2 + 0.0156X_5^2 \end{aligned} \quad (5)$$

where R_1 and R_2 are the degradation efficiency of MB and MV dyes in a binary mixture of dyes. Figure 5 illustrates the correlation between predicted and experimental MB and MV dye degradation efficiency. These plots show that all points are in a straight line and indicate a good correlation between predicted and actual values of degradation.

Three-dimensional response surface plots are used to demonstrate and analyze the combined effects of independent variables. They are also used to identify the major interactions between variables on photocatalytic

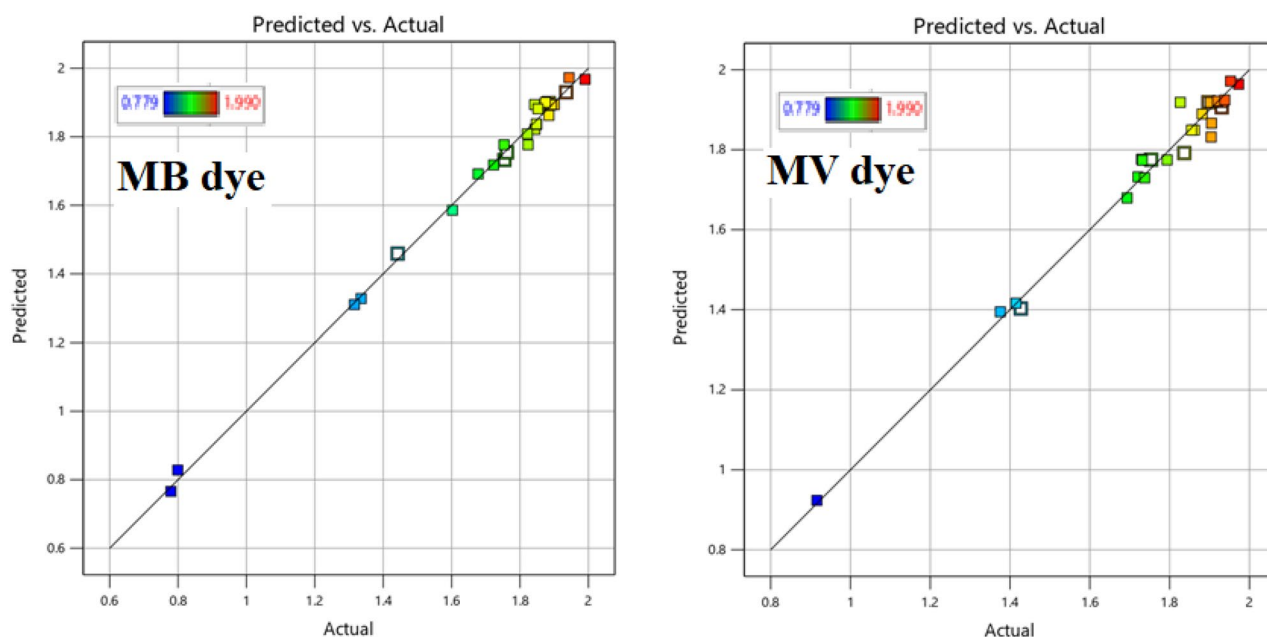


Figure 5. Predicted vs. actual photodegradation efficiency of (a) MB dye and (b) MV dye.

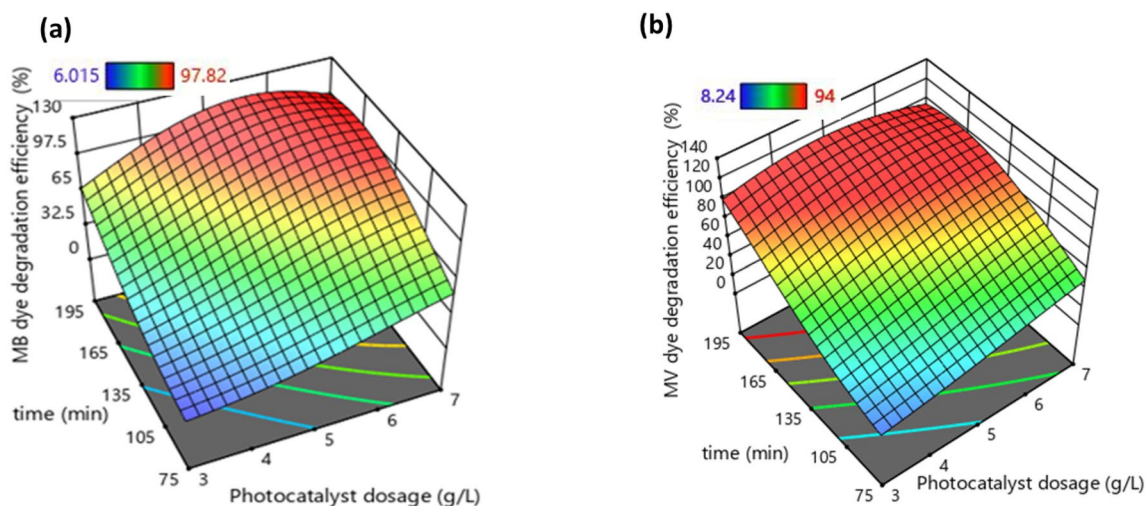


Figure 6. 3D plots showing the influence of photocatalyst dosage and period of photocatalysis reaction on (a) MB dye and (b) MV dye degradation efficiencies.

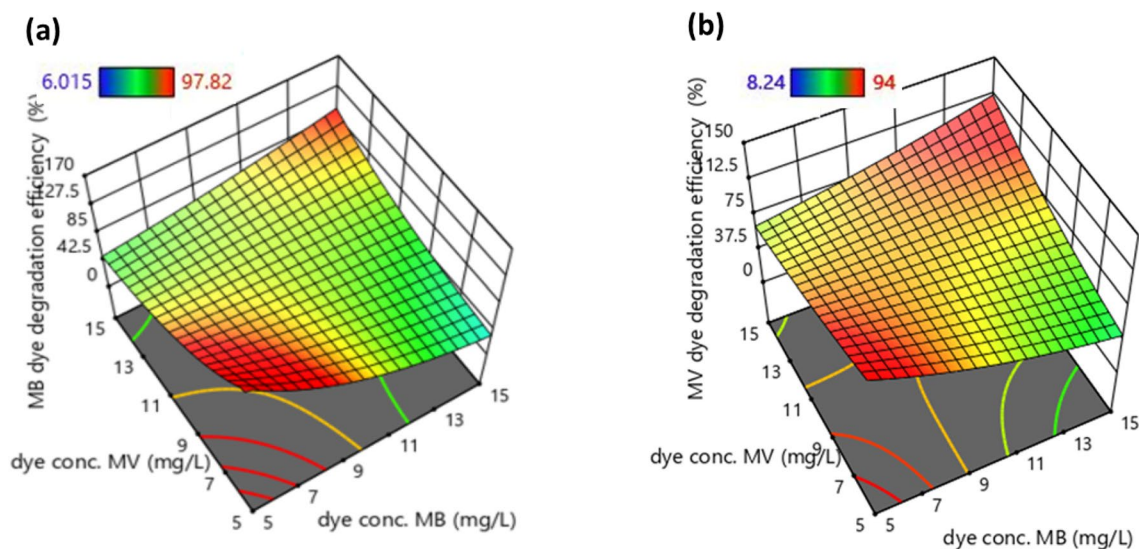


Figure 7. 3D plots showing the influence of concentrations of dyes on (a) MB dye and (b) MV dye degradation efficiencies.

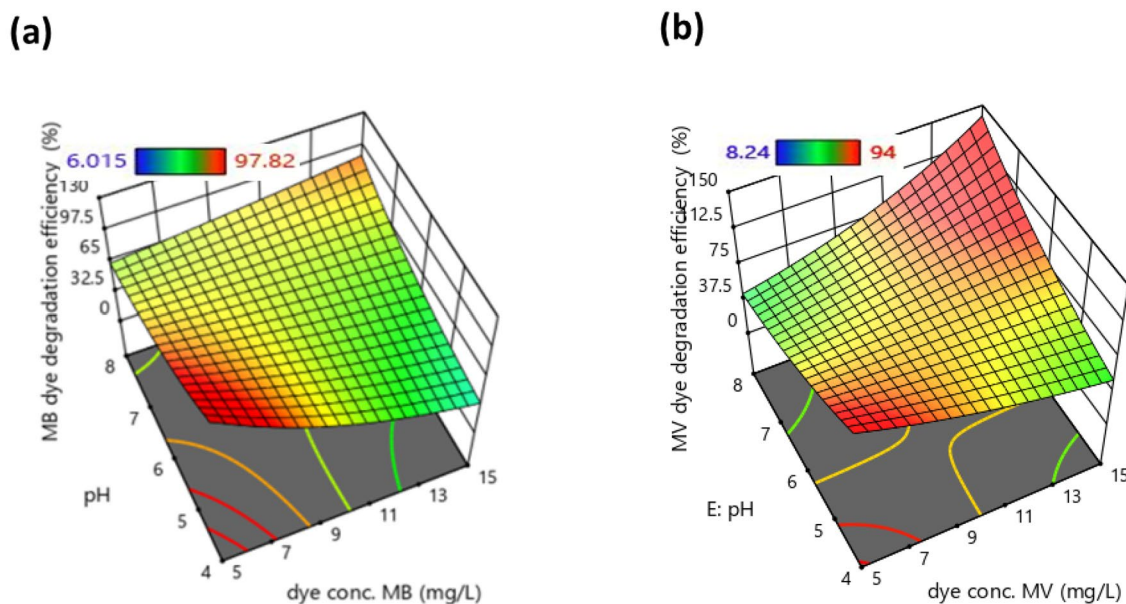


Figure 8. 3D plots showing the influence of pH of solution on (a) MB dye and (b) MV dye degradation efficiencies.

degradation. The three-dimensional (3D) surface response was plotted against two factors with other factors being constant (Figs. 6, 7, and 8).

Figure 6 shows the influence of irradiation time and photocatalyst dosage on photocatalytic activity in binary solution. Figure 6a specifically shows the behavior of MB dye degradation efficiency and the influence of these parameters. It is observed that irradiation time has a positive effect on degradation efficiency, which means as much as the irradiation time is high, degradation efficiency will be higher. Furthermore, photocatalyst dosage also has a similar positive effect on photocatalytic activity. Figure 6b shows the influence of photocatalyst dosage and irradiation time on the degradation efficiency of MV dye in binary solution. The influence of the discussed parameters is similar to the case of MB dye degradation efficiency. The positive influence of irrigation time is easily justified because it is similar to photocatalysis reaction time. However, the positive influence of photocatalyst dosage is due to increased surface area promoting the photocatalytic reaction by increasing radical generation⁵¹. On comparing both plots (Fig. 6 a and b) it is observed that photocatalyst dosage has a higher influence on the degradation activity of MV dye.

Figure 7 shows the influence of individual dye concentrations (MB and MV dye) in binary dye on photocatalytic activity. Figure 7a shows this influence, it can be observed that the MB dye degradation activity in binary solution is high when the individual dyes are very high or very low. Furthermore, when the concentrations of

individual dyes are very low, the degradation activity is greater than the activity of a highly concentrated binary solution. Similar types of observations are also seen in the case of individual MV dye degradation efficiency in the binary solution (Fig. 7b). This is because higher concentration leads to more dye molecules. The ratio of reaction sites to dye molecule is low which lowers the degradation efficiency in the predefined time range. Degradation efficiency will be higher if reaction time is high. The ratio of reaction sites and dye molecule is low when the initial concentration is low, which leads to high degradation efficiency⁵¹ When both are compared it is found that all influences are higher in the case of individual MV dye degradation efficiency in binary solution.

Figure 8, shows the influence of the pH of the dye binary solution. Figure 8a shows that the basicity of the solution supports the degradation activity of individual MB dye in binary solution. Whereas, an acidic solution is good for MV dye degradation activity in binary solution. This is because the compound effect of surface electrical charge characteristics of the catalyst dictates the ionization state of the catalyst surface⁵².

The degradation of dyes was optimized for constraints shown in Table 5. As indicated in the table the degradation activity of both dyes in the binary solution is highly desirable.

These constraints and desirable were used to optimize the photocatalytic process through discussed software. This analysis results in Fig. 9. Figure 9 shows profiles of predicted values and desirability functions for degradation of MB and MV dyes in binary solution and indicates the levels of each variable (X1, X2, X3, X4, and X5) in the model and the degradation percentage and desirability function value. The results illustrated in Fig. 8 indicate that the maximum photodegradation of MB and MV using MgO powder as a photocatalyst is 99.36 and 97.29% when 6.76 g/L of catalyst is used for photocatalysis for 152 min while individual concentrates of MB and MV dyes are 8.21 mg/L and 11.8 mg/L respectively moreover the pH of binary solution is 6.43.

Optimization study suggested the value of parameters for high degradation efficiency. These values were used for the validation of the optimization study by experiments. The experiments were performed and the results are

Factor	Goal	Lower limit	Upper limit	Lower weight	Upper weight	Importance
X1: Photocatalyst dosage	In range	3	7	1	1	3
X2: Time	In range	75	195	1	1	3
X3: MB dye concentration	In range	5	15	1	1	3
X4: MV dye concentration	In range	5	15	1	1	3
X5: pH	In range	4	8	1	1	3
R1: MB dye degradation efficiency	target = 100	6	100	1	1	5
R2: MV dye degradation efficiency	target = 100	7.8	100	1	1	5

Table 5. Table of constraints for optimization of photocatalytic degradation of a binary mixture of dye.

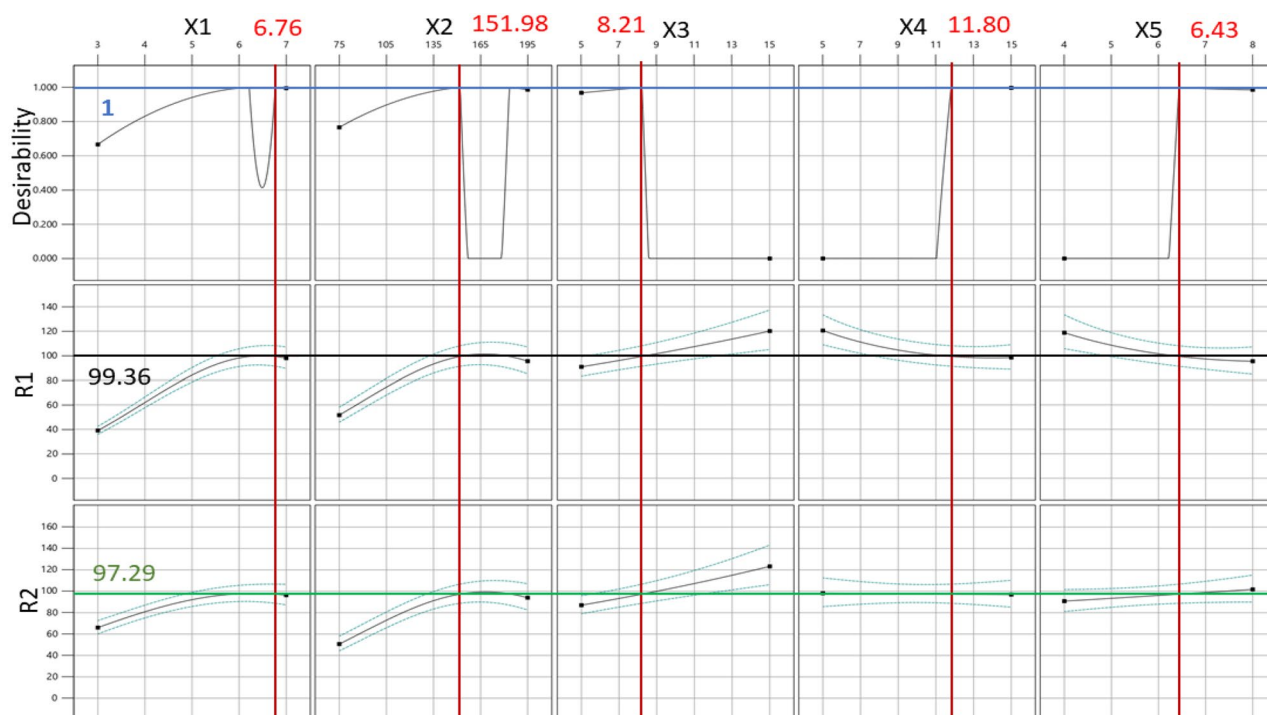


Figure 9. Profiles of desirability and photocatalysis degradation of binary dye mixture.

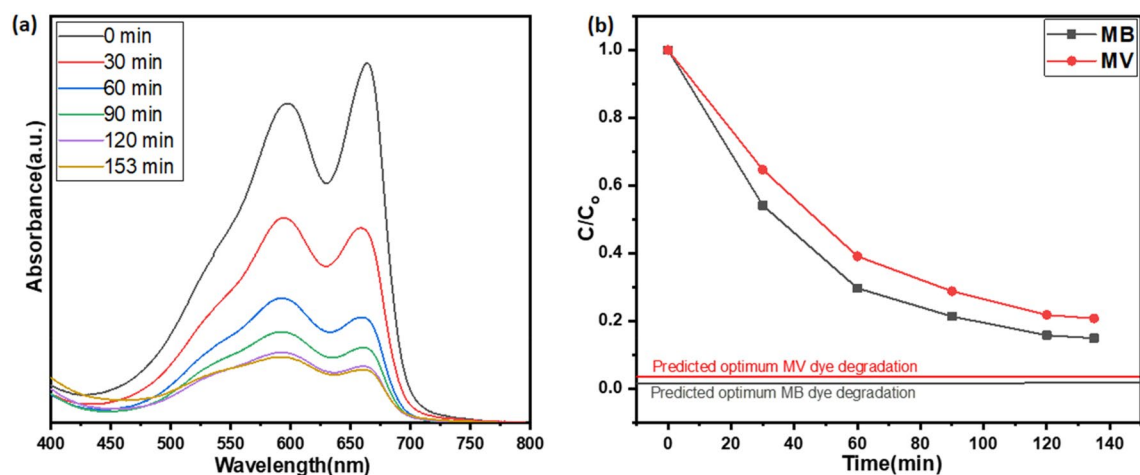


Figure 10. Photodegradation of a mixture of dyes at optimum parameter (a) UV- spectra, (b) C/C_0 vs. time.

Sr. No	Reference	MgO catalyst modification	Single/binary dye	Time (min)	Degradation activity
1	Naren et al. ⁵³	Phytochemically enriched MgO nanoparticles	Single dyes: Cationic-congo red dye and Anionic-malachite green dye	120	Congo red dye:95.8% Malachite green dye: 98.5%
2	Kurhade et al. ⁵⁴	No modification, MgO nanoparticles, green synthesis, optimization	Single dye: Nigrosine dye	200	96%
3	Kuruthukulangara et al. ⁵⁵	No modification, MgO nanoparticles	Single dye: Rhodamine B at pH 12	90	93.5%
4	Shkir et al. ⁵⁶	Ag loaded MgO	Single dye: Rhodamine B	120	MgO catalyst: 86%Ag loaded MgO: 91%
5	Barzegar et al. ⁵⁷	Phytoextract-mediated synthesis	Single dye: Methylene blue (MB)	120	87%
6	Liu et al. ⁵⁸	CuS and MgO loaded with S-doped biochar	Single dye: Rhodamine B	120	95.70%
7	Subalakshmi et al. ⁵⁹	$Cu_3(PO_4)_2/MgO$ nanocomposite	Single dye: Amaranth dye	150	98.8%
8	Zhou et al. ⁶⁰	Ternary ZnO-Sm ₂ O ₃ -MgO co-modified biochar	Single dye: Rhodamine B (RhB)	120	99.46%
9	Balakrishnan et al. ⁶¹	MgO nanoparticles	Single dye: Methylene blue (MB)	120	75%
10	Present work	MgO particles	Binary dye: Methylene blue (MB) and methylene violet (MV) dye	135	MB dye: 93%MV dye: 88%

Table 6. Comparative study of recently published research articles with present work.

displayed in Fig. 10. Photocatalytic degradation efficiency on optimum values is 85% and 80% for MB and MV dyes respectively in binary solution. Whereas predicted photocatalytic degradation efficiency is 99.36 and 97.29%. Absorption spectra (Fig. 10a) show that dyes are degrading. Figure 10b shows how MB and MV dyes degrade over time. Maximum photocatalytic degradation efficiency predicted by CCD is marked as a line in Fig. 10b. It can be seen that values are in close agreement with the predicted values. Table 6 shows the comparative study of recently published research articles related to the photocatalysis of textile dye through MgO as a catalyst material. None of the research articles was found related to the binary dye degradation through MgO photocatalyst.

Conclusions

MgO showed high photodegradation efficiency with both MB and MV dyes. The photocatalysis activity of a binary mixture of MB and MV dyes was also examined. MgO shows remarkable photodegradation efficiency of 97% and 88% for MB and MV dye respectively in a binary solution of dyes. The dye mixture degradation reaction follows first-order reaction kinetics according to the L–H model. The influence of process parameters was also evaluated with the help of CCD based on response surface methodology. Five factors (photocatalyst dosage (g/L), time of exposure (min), MB dye initial concentration (mg/L), MV dye initial concentration (mg/L), and pH of the dye solution) were selected for the study. The CCD technique suggested a minimum number of experiments to study the interaction of parameters. The CCD suggested 27 experiments to observe the influence of these parameters on photodegradation. These experiments were performed and the influence was evaluated. Experimental results were fitted to \log_{10} transformation of a polynomial to observe the influence. This study suggested that photocatalytic dosage and irradiation time have a positive influence on photocatalytic activity. Whereas the initial concentration of both dyes and pH of binary dye solution has such an influence that the photocatalytic activity is highest at the highest and lowest values. The photocatalytic process was also optimized for maximum photodegradation efficiency by CCD. The CCD suggested optimum values for parameters: photocatalyst dosage of 6.76 g/L, time of exposure of 151 min, MB dye initial concentration of 8.2 mg/L, MV dye initial concentration of 11.80 mg/L, and pH of 6.4. Furthermore, CCD suggested 99.36 and 97.29% of photodegradation efficiencies

for MB and MV dyes respectively on optimum parameters. Experiments were also conducted on optimum values suggested by CCD to validate optimization. The validation experiment showed 85 and 80% photodegradation efficiencies for MB and MV dye in binary solution. It can be seen that the values are in close agreement with the predicted values.

Data availability

The datasets used and/or analyzed during the current study are available from the corresponding author upon reasonable request.

Received: 24 October 2023; Accepted: 11 March 2024

Published online: 24 April 2024

References

- Slokar, Y. M. & Majcen Le Marechal, A. Methods of decoloration of textile wastewaters. *Dyes Pigm.* **37**(4), 335–356. [https://doi.org/10.1016/S0143-7208\(97\)00075-2](https://doi.org/10.1016/S0143-7208(97)00075-2) (1998).
- Wang, Z., Chen, Y., Xie, P., Shang, R. & Ma, J. Removal of *Microcystis aeruginosa* by UV-activated persulfate: Performance and characteristics. *Chem. Eng. J.* **300**, 245–253. <https://doi.org/10.1016/j.cej.2016.04.125> (2016).
- Yagub, M. T., Sen, T. K., Afroz, S. & Ang, H. M. Dye and its removal from aqueous solution by adsorption: A review. *Adv. Colloid Interface Sci.* **209**, 172–184. <https://doi.org/10.1016/j.cis.2014.04.002> (2014).
- Song, Z., Williams, C. J. & Edyvean, R. G. J. Treatment of tannery wastewater by chemical coagulation. *Desalination* **164**(3), 249–259. [https://doi.org/10.1016/S0011-9164\(04\)00193-6](https://doi.org/10.1016/S0011-9164(04)00193-6) (2004).
- Elazzouzi, M., El Kasmi, A., Haboubi, K. & Elyoubi, M. S. A novel electrocoagulation process using insulated edges of Al electrodes for enhancement of urban wastewater treatment: Techno-economic study. *Process Saf. Environ. Protect.* **116**, 506–515. <https://doi.org/10.1016/j.psep.2018.03.006> (2018).
- Verma, A. K., Dash, R. R. & Bhunia, P. A review on chemical coagulation/flocculation technologies for removal of colour from textile wastewaters. *J. Environ. Manag.* **93**(1), 154–168. <https://doi.org/10.1016/j.jenvman.2011.09.012> (2012).
- Wang, S., Wang, Z. & Zha, Z. Metal nanoparticles or metal oxide nanoparticles, an efficient and promising family of novel heterogeneous catalysts in organic synthesis. *Dalton Trans.* **43**, 9363. <https://doi.org/10.1039/b913539a> (2009).
- Teske, S. & Detweiler, C. The biomechanisms of metal and metal-oxide nanoparticles interactions with cells. *Int. J. Environ. Res. Public Health* **12**(2), 1112–1134. <https://doi.org/10.3390/ijerph120201112> (2015).
- Han, F., Kambala, V. S. R., Srinivasan, M., Rajarathnam, D. & Naidu, R. Tailored titanium dioxide photocatalysts for the degradation of organic dyes in wastewater treatment: A review. *Appl. Catal. Gen.* **359**(1–2), 25–40. <https://doi.org/10.1016/j.apcata.2009.02.043> (2009).
- Lee, K. M., Lai, C. W., Ngai, K. S. & Juan, J. C. Recent developments of zinc oxide based photocatalyst in water treatment technology: A review. *Water Res.* **88**, 428–448. <https://doi.org/10.1016/j.watres.2015.09.045> (2016).
- DePuccio, D. P., Botella, P., O'Rourke, B. & Landry, C. C. Degradation of methylene blue using porous WO₃, SiO₂–WO₃, and their Au-loaded analogs: Adsorption and photocatalytic studies. *ACS Appl. Mater. Interfaces* **7**(3), 1987–1996. <https://doi.org/10.1021/am507806a> (2015).
- Simeonidis, K., Mourdikoudis, S., Kaprara, E., Mitras, M. & Polavarapu, L. Inorganic engineered nanoparticles in drinking water treatment: A critical review. *Environ. Sci.* **2**(1), 43–70. <https://doi.org/10.1039/C5EW00152H> (2016).
- Mantilaka, M. M. M. G. P. G., De Silva, R. T., Ratnayake, S. P., Amaratunga, G. & de Silva, K. M. N. Photocatalytic activity of electrospun MgO nanofibres: Synthesis, characterization and applications. *Mater. Res. Bull.* **99**, 204–210. <https://doi.org/10.1016/j.materresbull.2017.10.047> (2018).
- Raveesha, H. R. *et al.* The electrochemical behavior, antifungal and cytotoxic activities of phytofabricated MgO nanoparticles using *Withania somnifera* leaf extract. *J. Sci. Adv. Mater. Devices* **4**(1), 57–65. <https://doi.org/10.1016/j.jsamd.2019.01.003> (2019).
- Dong, Q. *et al.* Cytotoxic effects of MgO nanoparticles on human umbilical vein endothelial cells in vitro. *IET Nanobiotechnol.* **5**(2), 36–40. <https://doi.org/10.1049/iet-nbt.2010.0022> (2011).
- Bai, Z. *et al.* Development of a trapezoidal MgO catalyst for highly-efficient transesterification of glycerol and dimethyl carbonate. *CrystEngComm* **20**(29), 4090–4098. <https://doi.org/10.1039/C8CE00808F> (2018).
- Leung, Y. H. *et al.* Mechanisms of antibacterial activity of MgO: Non-ROS mediated toxicity of MgO nanoparticles towards *Escherichia coli*. *Small* **10**(6), 1171–1183. <https://doi.org/10.1002/smll.201302434> (2014).
- Vesely, D., Kalendová, A. & Němec, P. Properties of organic coatings depending on chemical composition and structure of pigment particles. *Surf. Coat. Technol.* **204**(12–13), 2032–2037. <https://doi.org/10.1016/j.surfcoat.2009.11.005> (2010).
- Bouafia, A. *et al.* The recent progress on silver nanoparticles: synthesis and electronic applications. *Nanomaterials* **11**(9), 2318. <https://doi.org/10.3390/nano11092318> (2021).
- Salehifar, N., Zarghami, Z. & Ramezani, M. A facile, novel and low-temperature synthesis of MgO nanorods via thermal decomposition using new starting reagent and its photocatalytic activity evaluation. *Mater. Lett.* **167**, 226–229. <https://doi.org/10.1016/j.matlet.2016.01.015> (2016).
- Bagheri, A. G. H., Sabbaghan, M. & Mirgani, Z. A comparative study on properties of synthesized MgO with different templates. *Spectrochim. Acta Mol. Biomol. Spectrosc.* **137**, 1286–1291. <https://doi.org/10.1016/j.saa.2014.08.059> (2015).
- Sathyamoorthy, R., Mageshwari, K., Mali, S. S., Priyadarshini, S. & Patil, P. S. Effect of organic capping agent on the photocatalytic activity of MgO nanoflakes obtained by thermal decomposition route. *Ceram. Int.* **39**(1), 323–330. <https://doi.org/10.1016/j.ceramint.2012.06.028> (2013).
- Mageshwari, K., Mali, S. S., Sathyamoorthy, R. & Patil, P. S. Template-free synthesis of MgO nanoparticles for effective photocatalytic applications. *Powder Technol.* **249**, 456–462. <https://doi.org/10.1016/j.powtec.2013.09.016> (2013).
- Guo, M. Y., Ng, A. M. C., Liu, F., Djurišić, A. B. & Chan, W. K. Photocatalytic activity of metal oxides—The role of holes and OH radicals. *Appl. Catal.* **107**(1–2), 150–157. <https://doi.org/10.1016/j.apcatb.2011.07.008> (2011).
- Lu, D. *et al.* Facile one-pot fabrication and high photocatalytic performance of vanadium doped TiO₂-based nanosheets for visible-light-driven degradation of RhB or Cr(VI). *Appl. Surf. Sci.* **359**, 435–448. <https://doi.org/10.1016/j.apsusc.2015.10.138> (2015).
- Pitre, S. P., McTiernan, C. D. & Scaiano, J. C. Library of cationic organic dyes for visible-light-driven photoredox transformations. *ACS Omega* **1**(1), 66–76. <https://doi.org/10.1021/acsomega.6b00058> (2016).
- Kaviyarasu, K. *et al.* Solution processing of CuSe quantum dots: Photocatalytic activity under RhB for UV and visible-light solar irradiation. *Mater. Sci. Eng.* **210**, 1–9. <https://doi.org/10.1016/j.mseb.2016.05.002> (2016).
- Wang, Y. *et al.* Fabrication of TiO₂ (B)/anatase heterophase junctions in nanowires via a surface-preferred phase transformation process for enhanced photocatalytic activity. *Chinese J. Catal.* **39**(9), 1500–1510. [https://doi.org/10.1016/S1872-2067\(18\)63096-7](https://doi.org/10.1016/S1872-2067(18)63096-7) (2018).
- Nipane, S. V., Korake, P. V. & Gokavi, G. S. Graphene-zinc oxide nanorod nanocomposite as photocatalyst for enhanced degradation of dyes under UV light irradiation. *Ceram. Int.* **41**(3), 4549–4557. <https://doi.org/10.1016/j.ceramint.2014.11.151> (2015).

30. Wang, K. *et al.* Highly efficient photodegradation of RhB–MO mixture dye wastewater by Ag₃PO₄ dodecahedrons under acidic condition. *J. Mol. Catal. Chem.* **393**, 302–308. <https://doi.org/10.1016/j.molcata.2014.06.026> (2014).
31. Liu, S., Liu, C., Wang, W., Cheng, B. & Yu, J. Unique photocatalytic oxidation reactivity and selectivity of TiO₂–graphene nanocomposites. *Nanoscale* **4**(10), 3193. <https://doi.org/10.1039/c2nr30427a> (2012).
32. Kumaraguru, K., Saravanan, P., Rajeshkannan, R. & Saravanan, V. A systematic analysis of hexavalent chromium adsorption and elimination from aqueous environment using brown marine algae (*Turbinaria ornata*). *Biomass Conv. Bioref.* **13**(9), 8223–8238. <https://doi.org/10.1007/s13399-021-01795-1> (2023).
33. Rajeshkannan, R., Rajasimman, M. & Rajamohan, N. Optimization, equilibrium and kinetics studies on sorption of acid blue 9 using brown marine algae *Turbinaria conoides*. *Biodegradation* **21**(5), 713–727. <https://doi.org/10.1007/s10532-010-9337-0> (2010).
34. Nasiri Azad, F. *et al.* Enhanced simultaneous removal of malachite green and safranin O by ZnO nanorod-loaded activated carbon: Modeling, optimization and adsorption isotherms. *N. J. Chem.* **39**(10), 7998–8005. <https://doi.org/10.1039/C5NJ01281C> (2015).
35. Ghaedi, M. *et al.* Modeling of competitive ultrasonic assisted removal of the dyes—Methylene blue and Safranin-O using Fe₃O₄ nanoparticles. *Chem. Eng. J.* **268**, 28–37. <https://doi.org/10.1016/j.cej.2014.12.090> (2015).
36. Dasthian, K., Porhmat, S., Rezvani, A. R., Ghaedi, M. & Sabzehmeidani, M. M. Adsorption of semisoft pollutants onto Bi₂S₃/Ag₂S-AC under the influence of ultrasonic waves as external field. *J. Ind. Eng. Chem.* **60**, 390–400. <https://doi.org/10.1016/j.jiec.2017.11.026> (2018).
37. Asfaram, A., Ghaedi, M., Hajati, S. & Goudarzi, A. Ternary dye adsorption onto MnO₂ nanoparticle-loaded activated carbon: Derivative spectrophotometry and modeling. *RSC Adv.* **5**(88), 72300–72320. <https://doi.org/10.1039/C5RA10815B> (2015).
38. Hossain, M. B. *et al.* Optimization of ultrasound assisted extraction of antioxidant compounds from marjoram (*Origanum majorana* L.) using response surface methodology. *Ultrason. Sonochem.* **19**(3), 582–590. <https://doi.org/10.1016/j.ultsonch.2011.11.001> (2012).
39. Asfaram, A., Ghaedi, M., Goudarzi, A. & Rajabi, M. Response surface methodology approach for optimization of simultaneous dye and metal ion ultrasound-assisted adsorption onto Mn doped Fe₃O₄-NPs loaded on AC: Kinetic and isothermal studies. *Dalton Trans.* **44**(33), 14707–14723. <https://doi.org/10.1039/C5DT01504A> (2015).
40. Akbari, S., Moussavi, G. & Giannakis, S. Efficient photocatalytic degradation of ciprofloxacin under UVA-LED, using S, N-doped MgO nanoparticles: Synthesis, parametrization and mechanistic interpretation. *J. Mol. Liq.* **324**, 114831. <https://doi.org/10.1016/j.molliq.2020.114831> (2021).
41. Panchal, P. *et al.* Eco-friendly synthesis of Ag-doped ZnO/MgO as a potential photocatalyst for antimicrobial and dye degradation applications. *Coord. Chem. Rev.* **493**, 215283. <https://doi.org/10.1016/j.ccr.2023.215283> (2023).
42. Fakhri-Mirzanagh, S., Ahadzadeh-Namin, K., Pirgholi Givi, G., Farazin, J. & Azizian-Kalandaragh, Y. The effect of capping agent on the structural, optical properties and photocatalytic activity of MgO nanostructures. *Physica Condens Matter* **583**, 412064. <https://doi.org/10.1016/j.physb.2020.412064> (2020).
43. Wang, H., Li, G. & Fakhri, A. Fabrication and structural of the Ag₂S-MgO/graphene oxide nanocomposites with high photocatalysis and antimicrobial activities. *J. Photochem. Photobiol.* **207**, 111882. <https://doi.org/10.1016/j.jphotobiol.2020.111882> (2020).
44. Tahir, M. Y., Sillanpaa, M., Almutairi, T. M., Mohammed, A. A. & Ali, S. Excellent photocatalytic and antibacterial activities of bio-activated carbon decorated magnesium oxide nanoparticles. *Chemosphere* **312**, 137327. <https://doi.org/10.1016/j.chemosphere.2022.137327> (2023).
45. Alaizeri, Z. M. *et al.* Facile synthesis characterization, photocatalytic activity, and cytotoxicity of ag-doped MgO nanoparticles. *Nanomaterials* **11**(11), 2915. <https://doi.org/10.3390/nano11112915> (2021).
46. Ahmad, A. *et al.* Bio-construction of MgO nanoparticles using Texas sage plant extract for catalytic degradation of methylene blue via photocatalysis. *Int. J. Environ. Sci. Technol.* **20**(2), 1451–1462. <https://doi.org/10.1007/s13762-022-04090-2> (2023).
47. Ananda, A. *et al.* Green synthesis of MgO nanoparticles using *Phyllanthus emblica* for evans blue degradation and antibacterial activity. *Mater. Today Proc.* **49**, 801–810. <https://doi.org/10.1016/j.matpr.2021.05.340> (2022).
48. Chen, J. *et al.* Optimization synthesis of carbon nanotubes-anatase TiO₂ composite photocatalyst by response surface methodology for photocatalytic degradation of gaseous styrene. *Appl. Catal.* **123–124**, 69–77. <https://doi.org/10.1016/j.apcatb.2012.04.020> (2012).
49. Sahoo, C. & Gupta, A. K. Optimization of photocatalytic degradation of methyl blue using silver ion doped titanium dioxide by combination of experimental design and response surface approach. *J. Hazard. Mater.* **215–216**, 302–310. <https://doi.org/10.1016/j.jhazmat.2012.02.072> (2012).
50. Soltani, R. D. C., Rezaee, A., Khataee, A. R. & Safari, M. Photocatalytic process by immobilized carbon black/ZnO nanocomposite for dye removal from aqueous medium: Optimization by response surface methodology. *J. Ind. Eng. Chem.* **20**(4), 1861–1868. <https://doi.org/10.1016/j.jiec.2013.09.003> (2014).
51. Kumar, P. & Vaish, R. Enhanced photocatalytic activity in BaBi₄Ti₄O₁₅ with excess Bi₂O₃. *Surf. Interfaces* **40**, 103082. <https://doi.org/10.1016/j.surf.2023.103082> (2023).
52. Hanafi, M. F. & Sapawe, N. Effect of pH on the photocatalytic degradation of remazol brilliant blue dye using zirconia catalyst. *Mater. Today Proc.* **31**, 260–262. <https://doi.org/10.1016/j.matpr.2020.05.746> (2020).
53. Naren Vidadar, T. M. *et al.* Surface chemistry of phytochemical enriched MgO nanoparticles for antibacterial, antioxidant, and textile dye degradation applications. *J. Photochem. Photobiol. Chem.* **448**, 115349. <https://doi.org/10.1016/j.jphotochem.2023.115349> (2024).
54. Kurhade, P. I., Mittal, S., Kodape, S. M. & Bhuyar, K. Optimization of photocatalytic removal of nigrosine dye using green synthesized MgO nanoparticles. *Biomass Convers. Bioref.* <https://doi.org/10.1007/s13399-024-05313-x> (2024).
55. Kuruthukulangara, N. & Asharani, I. V. Photocatalytic degradation of Rhodamine B, a carcinogenic pollutant, by MgO nanoparticles. *Inorg. Chem. Commun.* **160**, 111873. <https://doi.org/10.1016/j.inoche.2023.111873> (2024).
56. Shkir, M., AlAbdulaal, T. H., Manthrammel, M. A. & Khan, F. S. Novel MgO and Ag/MgO nanoparticles green-synthesis for antibacterial and photocatalytic applications: A kinetics-mechanism & recyclability. *J. Photochem. Photobiol. Chem.* **449**, 115398. <https://doi.org/10.1016/j.jphotochem.2023.115398> (2024).
57. Barzegar, M., Ahmadvand, D., Sabouri, Z. & Darroudi, M. Phytoextract-mediated synthesis of magnesium oxide nanoparticles using *Caccinia macranthera* extract and examination of their photocatalytic and anticancer effects. *Mater. Res. Bull.* **169**, 112514. <https://doi.org/10.1016/j.materresbull.2023.112514> (2024).
58. Liu, X. *et al.* Synergic effect of CuS and MgO for boosting adsorption-photocatalytic activity of S-doped biochar. *J. Phys. Chem. Solids* **185**, 111781. <https://doi.org/10.1016/j.jpcs.2023.111781> (2024).
59. Subalakshmi, A., Kavitha, B., Srinivasan, N., Rajarajan, M. & Suganthi, A. Evaluation of photocatalytic activity of Cu₃(PO₄)₂/MgO nanocomposite for the efficient removal of amaranth dye under solar light irradiation. *Inorg. Chem. Commun.* <https://doi.org/10.1016/j.inoche.2024.112033> (2021).
60. Zhou, Y. *et al.* Efficient adsorption-photocatalysis activity of ternary ZnO-Sm₂O₃-MgO co-modified biochar for dye removal. *Appl. Organomet. Chem.* <https://doi.org/10.1002/aoc.7349> (2024).
61. Balakrishnan, G., Velavan, R., Mujasam Batoo, K. & Raslan, E. H. Microstructure, optical and photocatalytic properties of MgO nanoparticles. *Results Phys.* **16**, 103013. <https://doi.org/10.1016/j.rinp.2020.103013> (2020).

Acknowledgements

The authors extend their appreciation to the Deanship of Scientific Research at King Khalid University, Saudi Arabia for funding this work through the Large Research Groups Program under grant number R.G.P2/586/44. This work was also supported by the Korea Institute of Energy Technology Evaluation and Planning (KETEP) and the Ministry of Trade, Industry & Energy (MOTIE) of the Republic of Korea (No. RS-2023-00236325). This work was also supported by the research fund of Hanyang University (HY-20200000000033).

Author contributions

Hyeong Kwang Benno Park did the photocatalytic experiments and Pushpendra Kumar did the RSM analysis. The manuscript was written by Pushpendra Kumar, Hyeong Kwang Benno Park, Imen Kebaili, and Imed Boukhris. Yun Hwan Joo, Tae Hyun Sung reviewed the manuscript. The conceptualization of research was done by Anuruddh Kumar.

Competing interests

The authors declare no competing interests.

Additional information

Correspondence and requests for materials should be addressed to A.K.

Reprints and permissions information is available at www.nature.com/reprints.

Publisher's note Springer Nature remains neutral with regard to jurisdictional claims in published maps and institutional affiliations.



Open Access This article is licensed under a Creative Commons Attribution 4.0 International License, which permits use, sharing, adaptation, distribution and reproduction in any medium or format, as long as you give appropriate credit to the original author(s) and the source, provide a link to the Creative Commons licence, and indicate if changes were made. The images or other third party material in this article are included in the article's Creative Commons licence, unless indicated otherwise in a credit line to the material. If material is not included in the article's Creative Commons licence and your intended use is not permitted by statutory regulation or exceeds the permitted use, you will need to obtain permission directly from the copyright holder. To view a copy of this licence, visit <http://creativecommons.org/licenses/by/4.0/>.

© The Author(s) 2024